Structural matching of ferroelectric domains and associated distortion in potassium titanyl phosphate crystals

2003 J. Phys.: Condens. Matter 15 1613

(http://iopscience.iop.org/0953-8984/15/10/310)

INSTITUTE OF PHYSICS PUBLISHING JOURNAL OF PHYSICS: CONDENSED MATTER

J. Phys.: Condens. Matter **15** (2003) 1613–1624 PII: S0953-8984(03)55524-2

Structural matching of ferroelectric domains and associated distortion in potassium titanyl phosphate crystals

P Pernot-Rejmánková[1], P A Thomas[2], P Cloetens[1], T Lyford[2] and J Baruchel[1]

[1] European Synchrotron Radiation Facility, BP 220, F-38043 Grenoble, France
[2] Department of Physics, University of Warwick, Coventry CV4 7AL, UK

E-mail: rejma@esrf.fr

Received 4 November 2002
Published 3 March 2003
Online at stacks.iop.org/JPhysCM/15/1613

Abstract

The surface deformation and atomic-level distortions associated with crystal structural matching at ferroelectric inversion domain walls are investigated in periodically poled potassium titanyl phosphate (KTP) crystals. A deformation, of the order of 10^{-8} m in scale and having the periodicity of the domains, is observed at the surfaces by optical interferometry. It is discussed in terms of the piezoelectric effect. The matching of the crystal structures at the domain walls is studied by combining the hard x-ray Fresnel phase-imaging technique with Bragg diffraction imaging methods ('Bragg–Fresnel imaging') and using synchrotron radiation. Quantitative analysis of the contrast of the Bragg–Fresnel images recorded as a function of the propagation distance is demonstrated to allow the determination of how the domains are matched at the atomic (unit cell) level, even though the spatial resolution of the images is on the scale of micrometres. The atom P(1) is determined as the linking atom for connecting the inversion domains across the wall in KTP crystals for domain walls forced by electric-field processing to be parallel to (100). In addition to this, it is shown that a shift of $1/2(\boldsymbol{a} + \boldsymbol{b})$ between atoms in the original and inverted structures is introduced as a result of the domain inversion operation.

(Some figures in this article are in colour only in the electronic version)

1. Introduction

Twin boundaries often occur in the low-temperature phase of crystalline solids undergoing a phase transition upon cooling, when the low-temperature structure can be derived from the high-temperature one through the loss of one or more symmetry operations. We are concerned

with a particular kind of twin boundary, which occurs in ferroelectric crystals and separates regions of opposite polarity. This is known as an inversion or 180° domain wall. Periodic arrays of such domain walls have been investigated in KTP crystals using:

(1) modern optical interferometric techniques to investigate the domain-associated distortion arising at the surfaces;
(2) highly coherent synchrotron x-ray beams for the study of the matching of the crystal structures of the domains at the atomic level.

The x-ray beams produced at third generation synchrotron radiation facilities are highly coherent because the angular size, α, of the source, as seen from a point in the specimen, is very small. This results from both the small electron beam section in the insertion device (some 10^{-5} m) and the long distance between the source and the sample (of the order of 10^2 m). It leads to a large lateral coherence length, $\ell_c = \lambda/2\alpha$, of the x-ray beam, where λ is the wavelength. The angular source size is in the μrad range on the imaging beam line ID19 of the ESRF, and hence ℓ_c is about 100 μm for $\lambda = 1$ Å. This makes it possible to reveal with great instrumental simplicity, using only the so-called 'propagation technique', the phase variations of hard x-rays [1, 2]. From the optical point of view, the effect that is used to change the local phase variations into intensity variations is interference at finite distances between parts of the beam that have suffered different phase shifts and are mutually coherent. It can be described in terms of Fresnel diffraction or, alternatively, as in-line holography.

In 1836, Talbot [3] pointed out a remarkable self-imaging Fresnel diffraction effect for periodic objects and visible light. He showed that, under spatially coherent quasi-monochromatic illumination of wavelength λ, the images of a periodic object, of period a, are also periodically repeated as a function of the object-to-detector distance, this new period being the Talbot distance $D_T = 2a^2/\lambda$ [4]. For instance, in the case of an *absorption*-based grating, for which the amplitude of the wave is modified by the transmission through the object, 'perfect' images of the object will be recorded at distances $D = nD_T/2$, for integer n even, and the same image, with just a lateral displacement of $a/2$, will be recorded at distances $D = mD_T/2$, for integer m odd.

Potassium titanyl phosphate ($KTiOPO_4$; KTP) is widely used for applications in non-linear optics, in particular for frequency doubling. Via a quasi-phase-matching technique [5], which utilizes periodic domain inversion to overcome the limitations imposed by ordinary birefringent phase matching, any frequency within the transparency window of a material can be doubled efficiently. KTP is a ferroelectric at room temperature (although the high conductivity shown by flux-grown crystals often prevents switching) with a crystal structure described by orthorhombic space group $Pna2_1$. The lattice parameters are [6]: $a = 12.819$ Å, $b = 6.399$ Å, $c = 10.584$ Å; the c axis being parallel to the direction of spontaneous polarization. KTP undergoes a ferroic transition to the paraelectric phase [6], space group $Pnan$, at the Curie temperature of 934 °C [7].

The principal aims of this study are to understand the structure of domain walls in KTP crystals and to demonstrate how coherent x-ray methods can give unique information about atomic arrangements at domain walls. A relatively new technique—*combined Bragg and Fresnel imaging*—which takes advantage of the coherence of the synchrotron x-ray beam, and was demonstrated first for $LiNbO_3$ crystals [8, 9], is employed. This technique has already been successfully applied to elucidate the atomic-level structure at the ferroelectric domain walls in $KTiOAsO_4$ (KTA) [10]. The domain walls in both the $LiNbO_3$ and KTA investigated previously and the KTP investigated here were deliberately introduced by the method of periodic poling. This means that the ferroelectric polarization (and the crystal structure) is inverted in alternate regions of the crystal by application of an electric field through periodic

electrodes. The period of the arrays of inversion domains produced is on the scale of several to tens of microns. Under illumination by x-rays of lateral coherence length considerably larger than the period of poling, the array of domains is a periodic object, which produces the Talbot effect. In general, neighbouring 'up' and 'down' domains differ in their x-ray scattering both through the amplitude and phase of the structure factors of the Friedel pair of reflections F_{hkl} and $F_{\bar{h}\bar{k}\bar{l}}$. However, by far the largest contribution to the contrast between the domains is produced by the difference in phase, which is principally structural in origin. It is by recovery of this 'phase jump', $\Delta\varphi$, across the domain wall and comparison of the measured jump with simulations using different structural models, that atomic-level information about the domain walls is elucidated. It is important to note that, when a periodically poled crystal is in the Bragg diffraction position for a spatially coherent x-ray beam, it behaves essentially as a *phase* grating. The Bragg-diffracted x-rays from adjacent ferroelectric domains exhibit a phase-shift, $\Delta\varphi$, when they leave the crystal. After free-space propagation, phase variations in the wave are transformed into intensity variations and at distances $D = mD_T/4$ (for integer m odd) perfect images of the phase grating are expected.

By investigating a periodic array of domains, it is possible to utilize the conformity with the Talbot effect to interpret the x-ray images since it is known how they should evolve as a function of crystal-to-film distance. Furthermore, by examining a number, n, of periods of domains and, therefore, a number $2n+1$ of inversion domain walls within the lateral coherence of the beam, the information from a single domain wall is amplified, in a similar way to the amplification of the diffraction signal from a single unit cell upon Bragg diffraction from the periodic crystal. Thus, whilst it is not essential for the method to have a periodic array of walls, it is seen to be an advantage for retrieving structural information, providing that the walls are sufficiently identical.

The value of $\Delta\varphi$ calculated from the crystal structure depends very sensitively on exactly how the crystal structures of the domains are matched or linked across the domain wall. From crystallographic principles, four possible domain-matching schemes have been suggested for KTP crystals [11, 12]. They correspond to the following symmetry operations: (1) n-glide plane perpendicular to the [001] direction passing through the Ti(1) atom; (2) operation 2[010] through the P(1) atom; (3) operation 2[100] through the P(2) atom; (4) inversion through the Ti(2) atom. A fifth possibility is also considered here, i.e. domain matching through the position of the inversion centre in the paraelectric phase, denoted by $\mathrm{Ti}(2)_{para}$. Each of these matching schemes introduces a different phase shift in Bragg diffraction from inverted domains. Therefore, by measuring the actual value of $\Delta\varphi$ and comparing it with values calculated with these various models, atomic-level information about the domain wall can be inferred.

2. Optical observation of the domain outcrop

2.1. Experimental details

Periodically poled samples of KTP were prepared by the low-temperature poling method at Tel Aviv University, using Z-cut wafers [13]. The periods of domain reversal, performed across the whole 0.5 mm thickness of the samples, were 9 and 24 μm. The domain walls were constrained by the poling mask to be normal to the [100] crystallographic direction.

Samples of KTP with artificially introduced inverted domains, either periodic or planar, were carefully polished and studied using an optical phase-shifting interferometer [14]. This apparatus allows precise mapping of the surface profile, with resolution of 1 Å in surface roughness and 1 μm in lateral position, by comparing different optical paths of the light reflected by the surface under investigation.

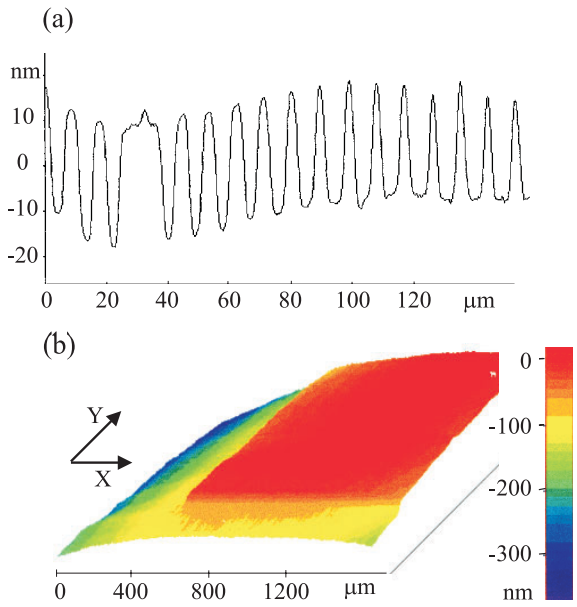

Figure 1. Surface profiles recorded using a phase-shifting interferometer of (a) a periodically poled KTP sample with 9 μm period. Valleys and hills correspond to 'up' and 'down' domains, respectively. Note an un-poled region on the left part of the graph. (b) A single domain KTP sample with one rectangular-shaped inversed domain. The 3D image corresponds to a region of the sample with a corner of the inverted domain (elevated part).

2.2. Results

Figure 1 summarizes the results of optical investigation for two different KTP crystals. Figure 1(a) shows the profile of a polished surface structure from a periodically poled KTP crystal with 9 μm period. The presence of steps around 30 nm height, with a period of 9 μm, is clearly visible. A similar surface profile was also found on the opposite surface of the sample. However, it was not possible to establish the correspondence of the surface modulations on opposite faces of the sample because of the small domain size. To determine this, a KTP sample having a large rectangularly shaped inverted domain, was studied (figure 1(b)). The 3D surface map shows that the inverted domain is elevated by approximately 80 nm with respect to the bulk in both the *X* and *Y* directions. On the opposite surface of the sample, this rectangular inverted domain is lowered by roughly the same amount with respect to the remaining part of the sample. A general conclusion can be made that the inverted domains are shifted in the *c* direction with respect to virgin crystal by tens of nanometres. It should be noted that the modulation of the surface remains almost unchanged, even after several consecutive re-polishings, or after depositing a thin aluminium film over the whole surface, thus eliminating the possibility that the surface steps observed could be an artefact brought about by modulation of the optical properties of the crystal. Similar periodic surface modulations were found in periodically poled samples of $LiNbO_3$ and KTA when investigated using this technique.

Figure 2 is an optical micrograph of the etched surface of a KTP crystal after a trial of periodic poling with domain walls normal to the [010] direction (24 μm period). It is seen from this image that the rate of domain growth normal to the [010] direction is much lower than that for domain growth normal to the [100] direction, resulting in irregularly shaped domains, an observation that agrees with the findings of Urenski *et al* [15].

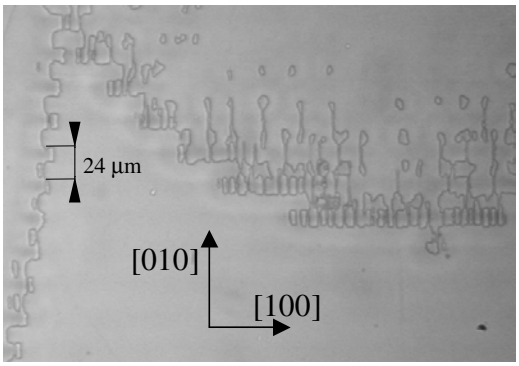

Figure 2. Optical micrograph in reflection of the etched surface of a KTP crystal after periodic poling with the period of 24 μm and domain walls normal to the [010] direction. A KTP crystal clearly 'prefers' domain walls normal to the [100] direction with respect to the [010] direction.

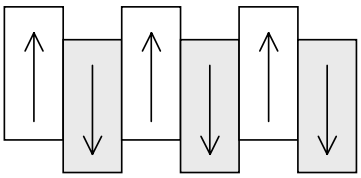

Figure 3. Periodically poled ferroelectric crystal: 'up' domains lifted with respect to 'down' ones leading to macroscopic surface steps. The arrows indicate the direction of spontaneous polarization.

2.3. Discussion

The combined results of the optical microscopy study of a variety of domain structures led to a picture of a domain-inverted sample as shown schematically in figure 3. The modulation of the surface height on opposing surfaces for the large rectangular domain proves that the relative movement of the inverted region is the same at both surfaces, i.e. it is as though the whole domain is systematically shifted parallel to [001] relative to the original crystal. Since the domains were produced by post-growth electric field processing, one possibility to consider is that piezoelectric strains generated during the domain inversion, and not fully relieved afterwards, are responsible for the modulation. However, an applied field E_3 along the [001] direction would produce a strain $\varepsilon_{33} = d_{333}E_3$ via the converse piezoelectric effect, where d_{333} is the piezoelectric coefficient, which would cause a region of the crystal subject to the field to expand at both surfaces (for d_{333} positive, as it is in KTP). Therefore, an inverted region should be elongated relative to and protrude beyond *both* surfaces, unlike the arrangement found experimentally and depicted in figure 3.

Further evidence against a processing-induced surface deformation model is provided by the observation that the surface modulation is preserved after several iterations of polishing after processing, thus suggesting that the deformations have a more intrinsic origin. Neighbouring domains possess surface charges of opposite signs, which are equal to their spontaneous polarizations and are of the order of ± 0.2 C m^{-2} in KTP, with the sign depending on the orientation of the domain. In displacing the surface of one domain relative to its neighbour of opposite polarity, the electrostatic energy of the arrangement is increased. However, the surface strain energy is correspondingly reduced by the deformation and a competition between

these effects, when properly evaluated, minimizes the energy at some equilibrium value of the surface step [16]. Importantly, this model predicts the correct behaviour of the steps on both surfaces of the crystal. The full calculation of this effect is currently in progress for publication elsewhere.

The anisotropy in the domain growth along [100] and [010] directions has been confirmed through optical examination of the failed attempt to produce a 24.7 μm grating with domain walls normal to the [010] direction (figure 2). The anisotropy of the domain growth has been explained by Urenski *et al* [15] on the Miller–Weinreich model [17], in which domains are assumed to progress sideways by discrete steps, with the minimum step being equal to the lattice parameter in a given direction. Since in KTP $a \approx 2b$, to a high degree of approximation, and the probability of a step is proportional to e^{-kl}, where l is the appropriate lattice parameter and k contains other constants, the factor of 10^2 is accounted for. It should further be noted that (100) walls may also be preferred structurally: Bierlein and Ahmed [18] suggested that, since a portion of the z-directed polarization consists of contributions of Ti–O chains oriented along the [011] and [0$\bar{1}$1] directions, the domain walls parallel to (100) planes, which do not intersect these chains, will be favoured.

The optical interference method utilized here has produced a *direct* visualization of the surface topology of inversion domains in KTP crystals, free from the effect of induced charges or potentials that can occur in other techniques, e.g. SEM [19] or the electron beam charging method [20]. Furthermore, this visualization technique does not rely on the interaction between the probe and the electric field of the domain wall, as in non-contact dynamic force microscopy [21], or upon the induced electrooptic effect at the walls, as in birefringent polarizing microscopy [22]. We suggest that the optical phase-shifting interferometer provides a powerful and informative method for the accurate investigation of the surface topology of ferroelectric domains, as demonstrated here.

3. Coherent x-ray imaging study of the domain matching

3.1. Experimental technique

The experiments were performed at the ID19 beam line of the ESRF. The basis of all diffraction imaging ('topography') techniques is to record the reflectivity variations within a Bragg spot and use this information to visualize the deformations and misorientations in the crystal under investigation. The image of a given Bragg spot corresponding to the projection of the whole (or a large part) sample on the film (or any other 2D detector) is a *projection topograph*. If the incident beam is restricted by a slit to a width of about 20 μm, only a virtual slice of the sample (as a first approximation) is investigated. The obtained image is a *section topograph*. Two simple set-ups designed to perform x-ray diffraction imaging were used: (a) in the white beam mode, projection topography in reflection; (b) in the monochromatic mode, section topography in transmission. The section and projection topographs were recorded on SR and HR Kodak Industrex films, respectively, with exposure times ranging from tens of seconds to a few minutes. The spatial resolutions of SR and HR films are approximately 5 and 1.5 μm, respectively.

3.2. Experimental results

A large number of reflections were investigated either in white or in monochromatic beam mode, using the projection or section topography technique, respectively. In what follows only two representative reflections are presented. Figure 4 shows white beam projection topographs

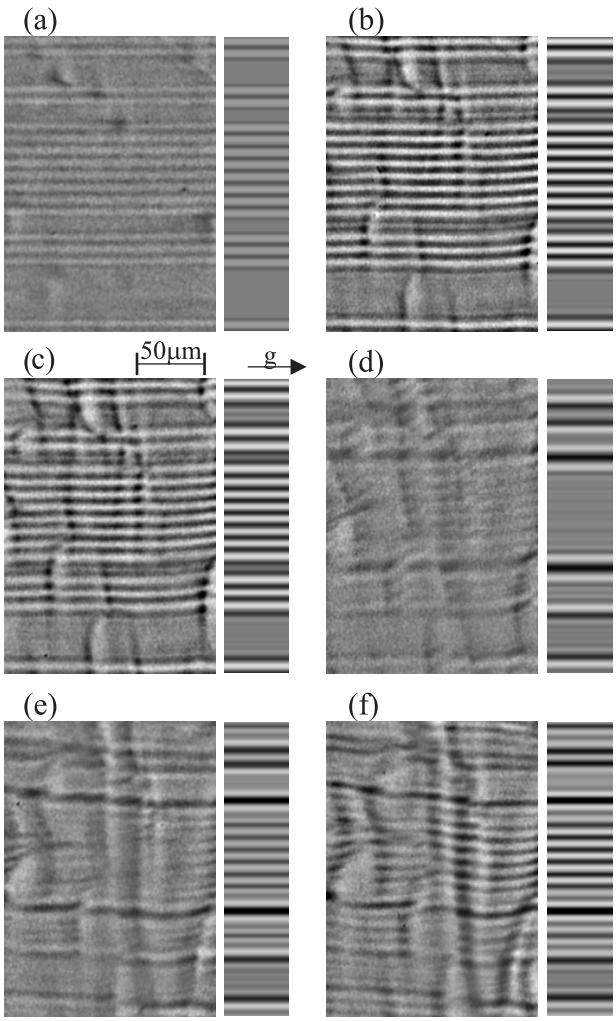

Figure 4. White beam projection topographs in reflection of a periodically poled KTP sample (9 μm period of poling) as a function of the defocusing distance D, using the 004 reflection, $\lambda = 0.788$ Å, higher harmonics being negligible. The contrast simulations are presented on the right side of each experimental image, considering $\Delta\phi = -38.6°$ (atom P(1) is supposed to be the origin; for details see the text). (a) $D = 0.107$ m, (b) $D = 0.568$ m, (c) $D = 0.697$ m, (d) $D = 1.023$ m, (e) $D = 1.18$ m, (f) $D = 1.382$ m; $\boldsymbol{g}$ is the projection of the diffraction vector on the detector.

in reflection of a 9 μm period KTP sample as a function of the defocusing distance D, using the 004 reflection. The defocusing distance is determined by the sample-to-detector distance d and the sample-to-source distance L (145 m in our case), and is equal to $D = d \cdot L/(d+L)$. The contrast simulations are presented on the right side of each experimental image, considering the phase shift, $\Delta\phi$ between structure factors of 004 and $00\bar{4}$ reflections equal to $-38.6°$. Note the very good agreement of interference fringes in experimental and simulated images not only at the regions of the sample where the poling was fully successful, but also at the regions, where the poling failed. A phase shift of $\Delta\phi = -38.6°$ is expected if the P(1) atom acts as a pivot atom for the twinning. The choice of the P(1) atom was confirmed to be the best fit

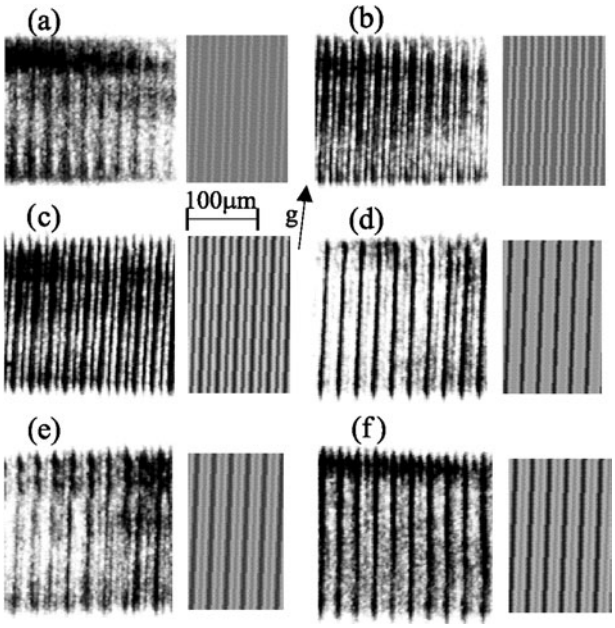

Figure 5. Monochromatic section topographs in transmission of a periodically poled KTP sample (24.7 μm period of poling) as a function of the defocusing distance D, using the 140 reflection, $\lambda = 0.75$ Å. The contrast simulations are presented on the right side of each experimental image, considering $\Delta\Phi = 180°$ ($1/2$ $(\boldsymbol{a} + \boldsymbol{b})$ shift between adjacent inversed unit cells is supposed; for details see the text) and the fraction b of the period where $\Delta\Phi$ is non-zero, equal to 0.454. (a) $D = 0.1$ m, (b) $D = 0.299$ m, (c) $D = 0.796$ m, (d) $D = 2.041$ m, (e) $D = 3.684$ m, (f) $D = 5.271$ m.

for most of the reflections. However, simply inverting the structure through P(1) as the origin does not provide a fit to all reflections. The most significant disagreement occurs for the $hk0$ reflections, for which the shift of the atomic positions in the c direction does not introduce any difference in the phases of the structure factors for the Friedel pair of reflections $hk0$ and $\bar{h}\bar{k}0$. Consequently, $\Delta\phi$ should be equal to 0 and no domain contrast should appear.

Figure 5 shows the set of monochromatic section topographs in transmission of a periodically poled KTP sample with 24.7 μm period as a function of the defocusing distance D, using the 140 reflection. The simulated images, presented on the right side of each experimental image, correspond to $\Delta\Phi = 180°$. A phase shift of 180° can be explained by a $1/2(\boldsymbol{a} + \boldsymbol{b})$ displacement between adjacent inverted unit cells in addition to the shift between adjacent domains in the c direction, which contributes zero to the phase jump for this reflection since $l = 0$. Note that, together with phase information, the Bragg-diffracted wave also contains intensity variations produced by crystal imperfections (such as dislocations) and, therefore, the resulting image is never a 'perfect' image of the grating. For this reason it is impossible to apply the same holographic reconstruction procedure as in Cloetens *et al* [23]. However, the evolving contrast from the periodic grating as a function of distance is sufficiently dominant in many regions of the crystal to allow the extraction of reliable structural data from the images.

In the model used to simulate the images of the 24.7 μm period KTP, the fraction b of the period where $\Delta\Phi$ is non-zero was set to $0.454a$, where a is the period of the domain inversion. This means that the 'up' and 'down' inversion domains are not of equal width but that one type is systematically thinner and occupies only 0.454 of the complete period. This departure of

the so-called *duty cycle* of the domains from the ideal 50:50 ratio was measured directly from the etched surfaces of the sample using a conventional optical microscope and was introduced to the model as an observed parameter.

All simulations, in both figures 4 and 5, were performed assuming $w = 0$, where w represents the fraction of the period over which the transition from one value of phase to the other occurs. This corresponds to an abrupt transition from $\Delta\varphi = 0$ to $\Delta\varphi \neq 0$ and models a change in structure from the original configuration to the inverted configuration across a single atomic layer. This represents the thinnest domain wall possible in structural terms.

3.3. Discussion

The comparison of the experimental and the simulated intensity variations, shown in figure 4, at different defocusing distances, allows the distinction to be made between the five possible domain-matching schemes, in which inversion domains are matched through the atoms Ti(1), P(1), P(2), Ti(2) and $\mathrm{Ti}(2)_{para}$, respectively. The phase shifts $\Delta\phi$ between adjacent domains were calculated for each model from the complex structure factors of the 004 Friedel pair; they are $-67.2°$, $-38.6°$, $-31.4°$, $-63.8°$ and $-59.2°$, respectively. The size and sign of $\Delta\phi$ depend strongly on the position of the origin for this calculation, i.e. which atom is placed at the position $z = 0$, with all other atoms in the unit cell being shifted by the requisite amount along the polar axis. The best fit to the observed modification of the contrast as a function of defocusing distance was obtained for $\Delta\phi = -38.6°$, i.e. P(1) being the pivoting atom for the twinning. This is consistent with our earlier results for domain-matching in $KTiOAsO_4$ (KTA), for which we found that the linking atom at (100) domain walls was the As(1) atom [10]. The 00ℓ reflections are sensitive only to the shifts between adjacent inverted unit cells in the c direction: any additional shifts along the a or b directions are not detected.

The experimental images in figure 5, which show the 140 reflection as a function of defocusing distance and for which there should be no domain contrast for atomic shifts only along the c direction, clearly suggest that there are also contributions to the phase shift in the a and/or b directions. This additional shift can be explained by the following structural argument. The domain inversion, or twinning, imparts to the combination of 'up' and 'down' structures (i.e. the periodically poled crystal) a higher effective symmetry, which mimics that of the high-temperature paraelectric phase and is described by space group $Pnan$. An atom located at a position (x, y, z) in one twin component (domain) has an equivalent atom at $(x + 1/2, y + 1/2, -z)$ in the other twin component (the inverted domain). The process of periodic domain inversion effectively reintroduces the n-glide symmetry operation that is lost in the paraelectric–ferroelectric phase transition from symmetry $Pnan$ to $Pna2_1$. It should be noted that this cannot be achieved by assuming that the n-glide plane passes through the pivot atom P(1), i.e. P(1) should not be conceived as the origin for the n-glide. Rather, the atomic shifts, which are assumed to be primarily along the $\boldsymbol{c}$ axis parallel to the applied poling field and occur relative to P(1) as the pivot atom, are such that an effective n-glide plane is introduced in its proper place in the structure, i.e. through Ti(1). The P(1) atom becomes the site of effective 2[010] symmetry in the quasi-$Pnan$ symmetry of the twinned structure, as shown in [11].

There are three types of reflection for Bragg–Fresnel imaging of (100) domain walls in KTP, as summarized in table 1. For a general reflection, the phase shift $\Delta\Phi$ produced by the translation $\boldsymbol{f}$ equal to $1/2$ $(\boldsymbol{a} + \boldsymbol{b})$, where $\boldsymbol{a}$ and $\boldsymbol{b}$ are lattice vectors, has to be added to the phase shift, $\Delta\phi$, produced by inversion of the z coordinate. The phase shift $\Delta\Phi$ is equal to $2\pi\boldsymbol{h}\boldsymbol{f}$ and leads to an integer multiple of 2π for all hkl reflections with $h + k = 2n$ (n integer), whereas $\Delta\Phi = (2n + 1)\pi$ if $h + k = 2n + 1$. In particular, for $hk0$ reflections, there are

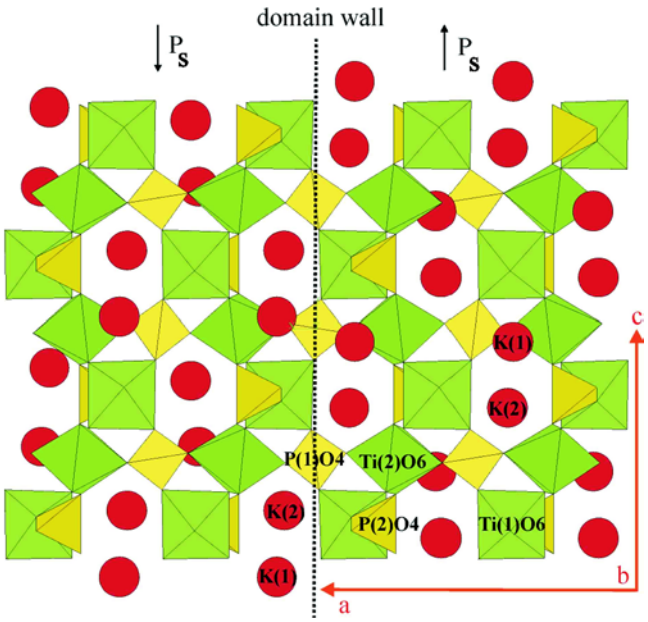

Figure 6. Schematic view of a domain wall (dotted line) perpendicular to the *a* axis passing through the atom P(1).

Table 1. Three types of reflections in Bragg–Fresnel imaging of (100) domain walls in KTP. The symbol $\Delta\varphi$ denotes the phase difference of the diffracted waves leaving the crystal, $\Delta\phi$ corresponds to the phase difference resulting from the displacement between adjacent inverted unit cells along the *c* direction and, finally, $\Delta\Phi$ is the phase difference (equal to 0° or 180°) produced by $1/2\,(\boldsymbol{a}+\boldsymbol{b})$ displacement.

Conditions on h, k and l	Phase shift $\Delta\varphi$	Examples for P(1) at origin
hkl, $h+k$ even, l unrestricted	$\Delta\phi$ only	004: $\Delta\varphi = \Delta\phi = 38.6°$
$hk0$, $h+k$ odd, $l=0$	$\Delta\Phi = \pi$ only	140: $\Delta\varphi = \Delta\Phi = \pi$
hkl, $h+k$ odd, l unrestricted	both $\Delta\phi$ and $\Delta\Phi$	162: $\Delta\varphi = \Delta\phi + \Delta\Phi = -30° + \pi = 150°$

two types: those with $h+k$ even, which are permitted in both the $Pnan$ and $Pna2_1$ phases, and those with $h+k$ odd, which are systematically absent in the $Pnan$ phase and present but weak (because of strong *n*-glide pseudo-symmetry) in the $Pna2_1$ phase. It is noted that the 140 reflection, which is particularly sensitive to the presence or absence of *n*-glide symmetry, shows strong contrast consistent with the π phase change brought about by the reintroduction of *n*-glide symmetry to the combined twin structure.

The model of twinning resulting from investigation by the Bragg–Fresnel imaging technique is shown in figure 6. The P(1) atom is the linking or pivot atom for connecting the inversion domains across the wall. Note that the continuity of the major structural chains of $P(1)O_4$–$Ti(2)O_6$ polyhedra along [100] is maintained across domain walls. The translation $1/2(\boldsymbol{a}+\boldsymbol{b})$ relates equivalent atoms in adjacent domains.

In general, the phase modulations of the Bragg-diffracted wave can have various origins. The modulations can be produced by regions with different structure factor phases, surface profiles or distortions of reflecting planes. A phase shift of a Bragg-diffracted wave will also be observed in the case that the distance between two regions (e.g. thickness of the boundary) is

not an integer multiplication of the cell parameter involved. For periodically domain-inverted crystals of the KTP family, our experiments suggest that the phase shifts of Bragg-diffracted waves are produced principally by the difference in phase, $\Delta\varphi$, of the structure factors of Friedel pairs of reflections in neighbouring domains. This allows the investigation only of microscopic shifts (smaller than the corresponding cell parameter) of atomic position in one cell of an 'up' domain with respect to the adjacent cell of a 'down' domain, as required for twinning. Any shifts between two domains corresponding to an integer multiple, n, of the lattice parameter introduce a phase shift of $2\pi n$, which is equivalent to a phase shift of zero. Therefore, deformations involving integer numbers of cell translations, either normal or parallel to the domain wall, are not detected using this technique.

The macroscopic periodic steps of 30 nm on the KTP sample surface introduce an additional phase shift of the Bragg-diffracted wave in reflection due to the different optical path lengths of x-rays incident upon a surface step up or down. Assuming that the total difference in surface height is an integral number of unit cells, this additional shift is calculated to be approximately $\pm 1^\circ$ for the wavelengths used and can be neglected compared with the large phase shifts, $\Delta\varphi$, introduced by Bragg diffraction.

4. Conclusion

The experimental determination of the domain wall structure is important for testing theoretical models of domain formation and for examining the conformity of the domain wall region, which can be considered as an interruption to long-range order, to the restrictions imposed by crystallographic symmetry. Surprisingly few techniques are available for examining ferroelectric domains on the spatial scales found in crystals. The Bragg–Fresnel imaging is unique in that detailed atomic-scale information about the wall region can be obtained relatively simply. The simulations of the experimental images obtained as a function of defocusing distance show that P(1) is the linking atom for connecting the inversion domains across the wall in KTP crystals with domain walls induced to be parallel to (100). In addition to this, it is found that equivalent atoms in adjacent domains are related by a $1/2(\boldsymbol{a} + \boldsymbol{b})$ translation consistent with the presence of n-glide symmetry in the resulting twin structure.

The topological surface profiles of the samples with inverted domains as directly measured using an optical interferometer show macroscopic shifts (of tens of nanometres) between 'up' and 'down' domains. These are suggested to result from a competition between electrostatic and strain energies at the crystal surfaces. The calculation concerning this model is in progress and will be published separately.

Acknowledgment

The authors wish to thank A Rommeveaux from ESRF Optic group, who performed the optical intereferometric measurements.

References

[1] Snigirev A, Snigireva I, Kohn V, Kuznetsov S and Schelokov I 1995 *Rev. Sci. Instrum.* **66** 5486
[2] Cloetens P, Barrett R, Baruchel J, Guigay J-P and Schlenker M 1996 *J. Phys. D: Appl. Phys.* **29** 133
[3] Talbot H F 1836 *Phil. Mag.* **9** 402
[4] Guigay J-P 1997 *Optics* **49** 121
[5] Armstrong J A, Bloemberegen N, Ducuing J and Pershan P S 1962 *Phys. Rev.* **127** 1918
[6] Thomas P A, Glazer A M and Watts B E 1990 *Acta Crystallogr.* B **46** 333

[7] Yanovskii V K and Voronkova V I 1980 *Phys. Status Solidi* a **93** 665
[8] Rejmánková-Pernot P, Cloetens P, Baruchel J, Guigay J-P and Moretti P 1998 *Phys. Rev. Lett.* **81** 3435
[9] Hu Z W, Thomas P A, Snigirev A, Snigireva I, Souvorov A, Smith P G R, Ross G W and Teat S 1998 *Nature* **392** 690
[10] Rejmánková-Pernot P, Thomas P A, Cloetens P, Lorut F, Baruchel J, Hu Z W, Urenski P and Rosenman G 2000 *J. Appl. Crystallogr.* **33** 1149
[11] Thomas P A and Glazer A M 1991 *J. Appl. Crystallogr.* **24** 968
[12] Liu W J, Jiang S S, Huang X R, Hu X B, Ge C Z, Wang J Y, Jiang J H and Wang Z G 1996 *Appl. Phys. Lett.* **68** 25
[13] Rosenman G, Skliar A, Eger D, Oron M and Katz M 1998 *Appl. Phys. Lett.* **73** 3650
[14] Whitehouse D J 1994 *Handbook of Surface Metrology* (Bristol: Institute of Physics Publishing) p 472
[15] Urenski P, Lesnykh M, Rosenwaks Y, Rosenman G and Molotskii M 2001 *J. Appl. Phys.* **90** 1950
[16] Rowlands G 2002 private communication
[17] Miller R and Weinreich G 1960 *Phys. Rev.* **117** 1460
[18] Bierlein J D and Ahmed F 1987 *Appl. Phys. Lett.* **51** 1322
[19] Aristov V and Kokhanchik L 1992 *Ferroelectrics* **126** 353
[20] Rosenman G, Skliar A, Lareah I, Angert N, Tseitlin M and Roth M 1996 *Phys. Rev.* B **54** 6222
[21] Lüthi R, Haefke H, Meyer K-P, Meyer E, Howald L and Güntherodt H-J 1993 *J. Appl. Phys.* **74** 7461
[22] Gopalan V and Gupta M C 1996 *J. Appl. Phys.* **80** 6099
[23] Cloetens P, Ludwig W, Baruchel J, Van Dyck D, Van Landuyt J, Guigay J-P and Schlenker M 1999 *Appl. Phys. Lett.* **75** 2912